Article

Polyelectrolyte Platforms with Copper Nanoparticles as a Multifunctional System Aimed at Healing Process Support

Agata Lipko , Anna Grzeczkowicz , Magdalena Antosiak-Iwańska , Marcin Strawski , Monika Drabik , Angelika Kwiatkowska , Ewa Godlewska , Ludomira H. Granicka *

Posted Date: 30 January 2024

doi: 10.20944/preprints202401.2054.v1

Keywords: polyelectrolyte layer coating; copper nanoparticles; human lung A549 cell line

Article

Polyelectrolyte Platforms with Copper Nanoparticles as a Multifunctional System Aimed at Healing Process Support

Agata Lipko [1], Anna Grzeczkowicz [1], Magdalena Antosiak-Iwańska [1], Marcin Strawski [2], Monika Drabik [1], Angelika Kwiatkowska [1], Ewa Godlewska [1] and Ludomira H. Granicka [1,*]

[1] Nalecz Institute of Biocybernetics and Biomedical Engineering, Polish Academy of Sciences, Trojdena 4 st., 02-109 Warsaw, Poland

[2] Laboratory of Electrochemistry, Faculty of Chemistry, University of Warsaw, 00-927 Warsaw, Poland;

* Correspondence: Ludomira Granicka, e-mail: lgranicka@ibib.waw.pl; phone: +48 22 592 59 00 address: Ks. Trojdena 4 st., 02-109 Warsaw, POLAND.;

Abstract: Purpose: The aim of the study is an approach to a nanocomposite with copper nanoparticles, constituting a bacteriostatic surface for maintaining the human lung cells' function. **Methods**: The polyelectrolyte layer coating with copper nanoparticles incorporated was designed. As a bacteriostatic factor, copper nanoparticles were applied as a colloidal solution of copper nanoparticles (ColloidCuNPs) and solution of copper nanoparticles (CuNPs). The influence of polyelectrolytes on selected Gram(+) and Gram(-) strains was examined. The function and morphology of the human adenocarcinoma A549 cell line of epithelial human lung cells cultured in the presence of nanocomposite layer coatings were evaluated. We applied fluorescence and scanning electron microscopies, as well as flow cytometry, for such studies. Furthermore, the layer coating material was characterized by AFM and SEM-EDX. **Results**: It was observed that polyelectrolytes polyethylenimine and poly-L-lysine do not induce proliferation of *E.coli* strain. On the other hand, it induces the proliferation of *S. aureus* strain. Due to CuNPs effectiveness against *E.coli* strain, CuNPs were selected for further research. The designed coatings at proper NPs share sustained the function of human lung cells cultured within 10 days of culture. The AFM and EDX characterization confirmed copper presence in the layer coating nanomaterial. The presence of CuNPs in polyethyleneimine-based nanocomposite deepens the bacteriostatic effect on E. coli compared with PEI alone. Meanwhile, incorporating CuNPs in PLL at share allowed A549 cell maintenance, did not exert a bacteriostatic influence on the examined strain. **Conclusion**: The platform based on polyelectrolytes incorporated with copper nanoparticles ensuring the growth and appropriate morphology of the human lung epithelial cells might be considered an element of the system components for medical devices for maintaining the human lung cells' function.

Keywords: polyelectrolyte layer coating; copper nanoparticles; human lung A549 cell line

1. Introduction

Scientists and engineers' efforts in constructing increasingly advanced biomaterials with a multifunctional profile are reflected in countless publications regarding new systems that support the regeneration of injured tissues and restore their function [1–3]. Nonetheless, the topic remains unfathomable despite the wide range of designed and reported structures and platforms. Undoubtedly, novel biomaterials with specific properties, especially those for biomedical applications designed to meet several stringent requirements, have revolutionized modern therapy methods. However, it is worth remembering that individual patients have various physiological characteristics, making each case unique [4]. Consequently, universal biomaterials, even highly advanced ones, do not ensure the same clinical results in different patients and do not guarantee therapeutic success. More and more voices suggest that the future should be associated with personalized therapies. Therefore, in the era of the increasing popularity of personalized health care aimed at improving the quality of patients' lives, it is essential to constantly expand the base of available biomaterials intended for contact with patients' tissue [4].

 doi:10.20944/preprints202401.2054.v1

Antibacterial activity is a crucial property of modern biomaterials as an element in medical device system components [5–7]. Simultaneously, expanding antibiotic resistance of pathogens increases the demand for exploring novel antimicrobial agents and unconventional therapeutical approaches (e.g., application of antimicrobial peptide Tet213 [8], honey [9]).

Due to their unique features, like catalytic properties, the ability to modify surfaces to change their characteristics, as well as their role in energy conversion and storage, metallic nanoparticles are a novel group of nanomaterials usable in many areas like medicine, pharmacy, and environmental protection [10,11]. Owing to their inhibitory and robust antimicrobial effects, metal nanoparticles are recognized as an antibiotic alternative [12], circumventing multi-resistant antibacterial infections. Among the metal and metal oxide nanoparticles supporting wound healing, the most commonly applied are zinc oxide [13], iron oxide [14], cerium oxide [15], titanium oxide [16], silver [17], gold [18], and copper (CuNPs) [6]. The last ones have especially received broad attention recently, as they are more accessible, eco-friendly, and cost-effective than silver and gold equivalents [19]. Moreover, studies show copper nanoparticles exhibit lower toxicity than silver nanoparticles [20,21]. Furthermore, nano-biomaterials with metallic nanoparticles, including copper-based NPs, have been developed to improve mechanical strength and involve antimicrobial activity [22]. An example of such materials reported to show antibacterial functionality against *S. aureus* might be polyelectrolyte-copper nanocomposite coatings with the poly(diallyldimethylammonium chloride) playing a role of a polycation, poly(sodium 4-styrenesulfonate)(PSS) used as a polyanion as well as negatively charged CuNPs [23].

It is worth noting that copper nanoparticles have the ability to penetrate both viruses and bacterial cell membranes directly, liquidating them by releasing oxygen and toxic factors for the microbes. In addition, it is also a crucial living element of various human metabolic pathways. Hence, tissue regeneration can be enhanced using copper [24].

The role of coppers in angiogenesis cannot be underestimated [25–27].

Successful restoration of the blood flow in the injured tissues and/or vascularization of the engineered grafts ensuring supplies of nutrients, chemicals, and oxygen is crucial for transforming damaged areas back to functional tissues, yet very difficult to obtain. The cellular mechanism underlying the induction of angiogenesis by Cu is still largely unknown; however, it is currently extensively studied [12]. Moreover, Cu was shown to positively affect the migration and adhesion of various cell types *in vitro*, providing biomaterial with the ability to restore tissue continuity [28,29].

There are approaches to the usage of Cu ions for bone engineering purposes. Some authors proposed the mesoporous structured scaffolds built of bioactive glass containing CuNPs. It is true to say that the obtained structure allowed for increased angiogenesis [30]. Some other authors reported the biocompatibility of Cu^{2+}-doped bioactive glass scaffolds for bone marrow mesenchymal stem cell maintenance and angiogenesis enhancement due to the induction of vascular endothelial growth factor secretion by Cu^{2+} [31].

Cu ions can be used to boot angiogenesis. The 3D collagen porous scaffolds involving CuNPs were reported to be constructed for osteomyelitis treatment purposes. Along with the angiogenesis-promoting and bone-forming enhancement, an inhibitory effect on *S. aureus* was observed [32].

Copper nanoparticles are applied for bactericidal activity induction in bone cement. However, it was observed, e.g., in the case of tested PMMA modified with copper nanoparticles, that together with the higher bactericidal effect, the pulp stem cells' viability was reduced [33].

It can be noted that Cu has been recognized as an antibacterial agent for a long time [34]. Recently, studies on different cells and organisms established lower cytotoxicity of Cu nanoparticles compared to Cu ions [35]. Such results indicate that nanoparticle form could favor steady, relatively low release of Cu ions, not reaching the threshold to activate mammalian oxidative pathways but still able to disrupt the integrity of bacterial cell walls and membranes. Consequently, an opportunity occurs to obtain highly biocompatible material with antimicrobial properties. These features also resulted in special attention currently paid to Cu nanoparticles in the context of bone and cartilage engineering as they have exhibited remarkable pro-osteogenic and pro-chondrogenic activity [27,36,37].

 doi:10.20944/preprints202401.2054.v1

Due to the CuNPs properties combining angiogenesis-promoting and bacterio-static effects, the application for regeneration processes is implied.

The vital role of copper as a trace mineral required for regeneration [38] has been examined in practice. Recently, for applications in clinical practice, the effectiveness of commercially available dressings containing silver nanoparticles was compared with dressings containing copper nanoparticles. It was concluded that applying bandages involving copper nanoparticles enhanced the healing of hard-to-heal wounds. At the same time, bandages with copper nanoparticles proved to be more efficient than dressings containing silver nanoparticles [39].

Epithelial injury often characterizes respiratory diseases. However, an imbalance of lung homeostasis does not always lead to dysfunction. The lungs have a significant response capacity to injury by reparation and replacement of damaged cells, with the epithelium playing a critical role in returning to homeostasis by coordinating tissue repair [40,41]. Therefore, as components of respiratory support devices, it is advisable to develop materials that do not cause damage to epithelium cells, have bacteriostatic properties, and promote healing.

The study aims to develop a platform combining healing and bacteriostatic properties as an element in system components for medical devices for maintaining human lung cell function.

2. Materials and Methods

2.1. Preparation of the Polyelectrolyte Layer Coatings

Copper nanopowder with particles of size 25 nm (CuNPs), (Merck/Sigma-Aldrich), and Copper Colloid (ColloidCuNPs) (Nano-Koloid, EU) at a concentration of 50 ppm was used in the study. Applied solutions:

- 50 ppm Copper Colloid from bulk solution was applied.
- 1000 ppm CuNPs solution was prepared from copper nanopowder and deionized water (MilliQ) with 0,1% Triton-X. The solution was sonicated in the sonication water bath for a total of 11 hours with proper intervals to avoid overheating of the solution.

The polyelectrolytes: poly-L-lysine hydrobromide (MW 15-30kD) (Sigma, USA), branched poly(ethyleneimine), analytical standard, Mn ~60,000, Mw750,000, 50% (w/v) in H_2O (Sigma-Aldrich, Germany) were applied in the study.

We designed and prepared membrane layers based on polyethyleneimine and poly-L-lysine. The primary layers, i.e., polyethyleneimine (PEI) and polylysine (PLL), were received from 1 mg/ml polyelectrolyte solutions in phosphate-buffered saline (PBS) (Biomed Lublin, Poland). To obtain the membranes incorporating CuNPs (polyethylenimine incorporating CuNPs (PEI-CuNPs) and polylysine incorporating CuNPs (PLL-CuNPs)), a 20 ppm or 200 ppm of CuNPs water solution was added to a 1 mg/ml solution of selected polyelectrolyte in PBS at a 1:1 ratio and stirred for 4 h at room temperature. Similarly, membranes incorporating ColloidCuNPs (i.e., polyethylenimine incorporating ColloidCuNPs (PEI-ColloidCuNPs) and polylysine incorporating CuNPs (PLL-ColloidCuNPs) were prepared. A bulk solution of ColloidCuNPs was added to a 1 mg/ml PBS solution of appropriate polyelectrolyte at a 1:1 ratio. Then, the solution was stirred at room temperature for 4 h. The studied membranes were collected in Table 1.

Membranes were placed on glass coverslips for evaluation in systems with cells.

Table 1. Studied membranes.

Membrane	CuNPs	ColloidCuNPs
Polyethyleneimine-based		
polyethyleneimine (PEI)	No	No
polyethylenimine incorporating CuNPs (PEI-CuNPs)	Yes	No
polyethylenimine incorporating ColloidCuNPs (PEI-ColloidCuNPs)	No	Yes

 doi:10.20944/preprints202401.2054.v1

poly-L-lysine-based		
polylysine (PLL)	No	No
polylysine incorporating CuNPs (PLL-CuNPs)	Yes	No
polylysine incorporating CuNPs (PLL-ColloidCuNPs)	No	Yes

2.2. Maintaining cell culture

Media: Fetal Bovine Serum, FBS (Sigma-Aldrich, EU), Ham's F12 Medium/Dulbecco's Modified Eagle's Medium, F12/DMEM (Gibco, Thermo Fisher Scientific, USA).

The human adenocarcinoma A549 cell line from the human lung was used in the reported studies. The cells were maintained in the Kaighn's Modification of Ham's F-12 Medium (F12-K medium) supplemented with 10% FBS (37 °C, 5% CO_2). When the cells reached a confluence of approximately 80%, the culture bottles were emptied of the medium to wash cells with PBS free of Ca^{2+} and Mg^{2+} and then trypsinize them. After trypsinization, cells ($1\times10^3/cm^2$) were positioned on the membranes deposited on the bottom of culture wells and maintained in culture medium for 10 days (5% CO_2, 37 °C). The cell function was verified with propidium iodide by flow cytometry and MTT test after 3, 6, and 10 days of culture. Moreover, we employed scanning electron microscopy (SEM) to verify the immobilized cells' morphology. The cells cultured without membrane for 10 days served as a negative control.

2.3. Cell's functioning evaluation

We employed flow cytometry measurements and the (3-4,5-dimethylthiazol-2-yl)-2,5-diphenyltetrazolium bromide assay (MTT) to evaluate cells' functioning and metabolic activity.

For MTT studies, cells were deposited on the membrane films and cultured for 3-, 6-, and 10 days, respectively. After the specified time, the 5 g/L MTT solution was introduced to the culture in a 1:10 medium dilution, followed by 2 hours of cell incubation at 37°C with 5% CO_2. Next, the solution was discarded. At the end, DMSO was added. The absorbance of a solution was measured by a spectrophotometer (HP 8452, EU) at 550 nm, preceded by 15 minutes of shaking.

2.4. Fluorescence Staining

The cells were immobilized on the membranes, previously deposited on glass coverslips for the fluorescence staining. Then, we fixed samples in the 4% paraformaldehyde (PFA) solution in PBS (20°C, 15 min) for fluorescence staining. The next step was cell membrane permeabilization. TRITON X100 detergent, which allows dyes to penetrate individual cells, was employed to achieve it. Then, the fluorochrome-conjugated phalloidin (obtained from the Amanita phalloides toxin), which stains filamentous actin, was introduced. To visualize single cells, we added the fluorochrome solution to them. In this case, the DAPI, specifically staining DNA, was applied. It should be noted that cell nuclei stained DAPI show blue fluorescence under UV light. Finally, the samples were washed in PBS and studied in an APX1000 fluorescence microscope (Olympus). The red phalloidin fluorescence (λ = 570 nm) and the cytoskeleton's blue DAPI one (λ = 460 -500 nm) were examined.

2.5. Scanning Electron Microscopy Analysis

The visualization of bacterial cells incubated in the presence of layer coatings was made by applying scanning electron microscopy (SEM). We performed our analysis using a TM 1000 device (Hitachi, Tokyo, Japan). Firstly, bacterial cells were incubated for 24 hours; then, we fixed them using 2.5% glutaraldehyde, followed by multiple rinsing with Milli Q water. Next, the specimens were deposited in 75.0% ethanol for 15 min. We repeat the procedure. After that, a 15-minute incubation of samples in 99.8% ethanol was performed. The samples were air-dried in a microscope measuring chamber in the next step.

2.6. SEM-EDX Studies

 doi:10.20944/preprints202401.2054.v1

Crossbeam 540X scanning electron microscope (Carl Zeiss Microscopy GmbH, Germany) with an X-FEG cathode was used for SEM-EDX characterization, whereas the X-MAXN spectrometer (Oxford Instrument, UK) operating at 15 keV was applied to collect the EDX maps.

It should be noted that samples were lyophilized before entering the microscope chamber.

2.7. Statistical Analysis

The standard statistical analysis was performed by applying Statistica 7.1 software. The standard deviations, mean values, and the significance of the difference were assessed, wherein values for $p < 0.05$ were presumed to be significant.

3. Results

3.1. The polyelectrolyte layer coatings' bacteriostatic effect evaluation

Selected polyelectrolytes were examined as a base of materials for cooperation with NPs for systems aimed at medical devices for maintaining human cells' function. The effect of PEI and PLL, which exhibit adhesive properties towards viruses [42], on bacterial strains of *S. aureus* and *E. coli* was examined.

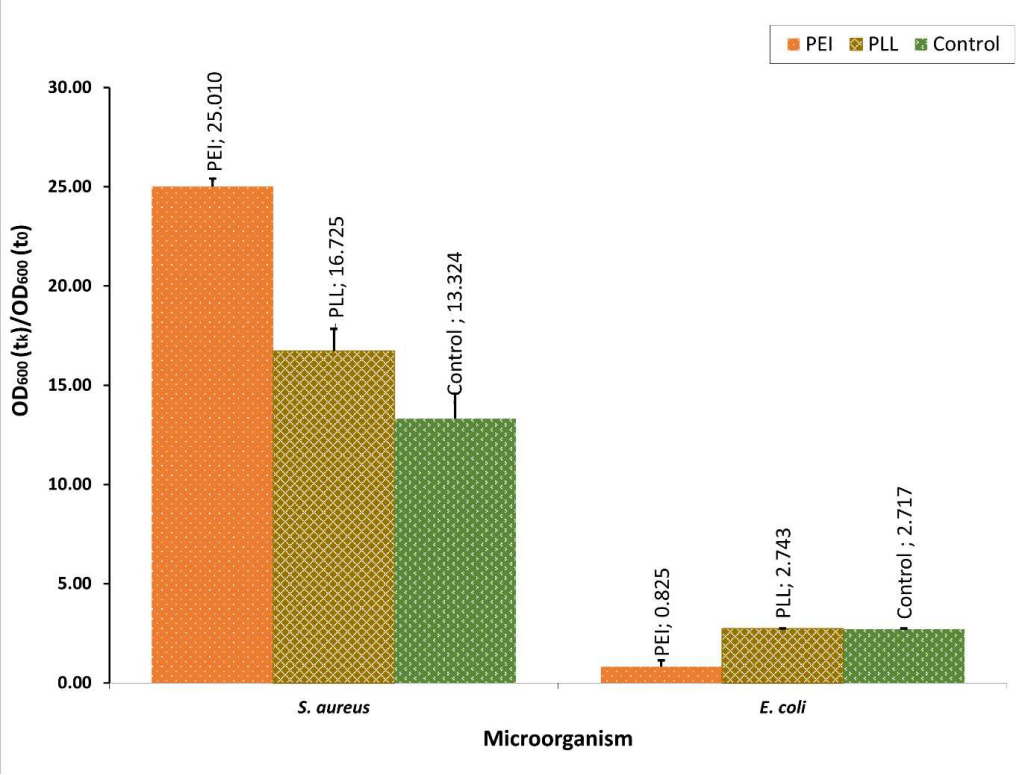

Figure 1. Bacterial strains optical density. Results for *S. aureus* and *E.coli* after 24-h culture in the presence of polyethyleneimine (PEI) and poly-L-lysine (PLL) layer coating are shown. The values are presented as mean ± SD. .

It can be seen that different materials have various effects on investigated strains. Assessing the bacteriostatic influence of the chosen polyelectrolytes demonstrated that they do not affect the strains Gram (+) and Gram (-) to the same extent. The performed assessment showed that PEI and PLL do not induce the proliferation of *E. coli*. Additionally, PEI showed a bacteriostatic effect on *E. coli*. A significant difference was noted in optical density compared to control. Furthermore, PLL does not affect the *E. coli* strain compared with control. As in au contraire, it was observed that the proliferation of *S. aureus* strains was higher after incubation in the presence of PLL and PEI polyelectrolytes (Figure

 doi:10.20944/preprints202401.2054.v1

1). The *E. coli* strain, whose proliferation was not induced by the abovementioned materials, was selected for further evaluation.

The SEM pictures of the selected strains after 24h incubation in the presence of evaluated layer coatings are presented in Figure 2.

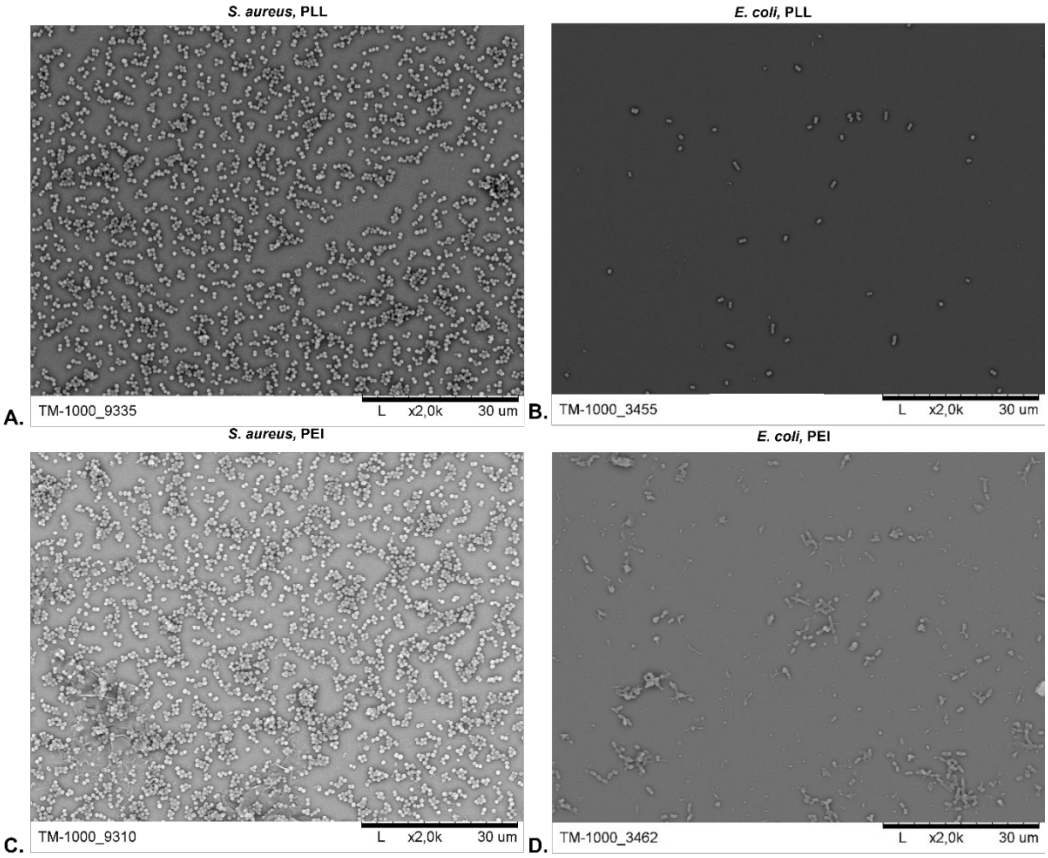

Figure 2. SEM picture of the strains *S. aureus, E. coli* after 24h incubation in the presence of coating layer PLL (A., B., respectively) and PEI (D., E., respectively).

3.2. Characterization of polyelectrolyte layer coatings

Atomic forces microscopy was applied to characterize the surface morphology and topography of the nanocomposite material samples. The ColloidCuNPs or CuNPs-incorporating layers were assessed. Moreover, the coating layers of chosen polyelectrolytes PLL and PEI nanoparticles incorporating were examined.

3.2.1. Surface topography analysis

It can be observed that the layer ColloidCuNPs exhibits a structure with densely marked centers over the entire surface. The layer CuNPs showed not densely, evenly marked centers over the entire surface (Figure 3).

 doi:10.20944/preprints202401.2054.v1

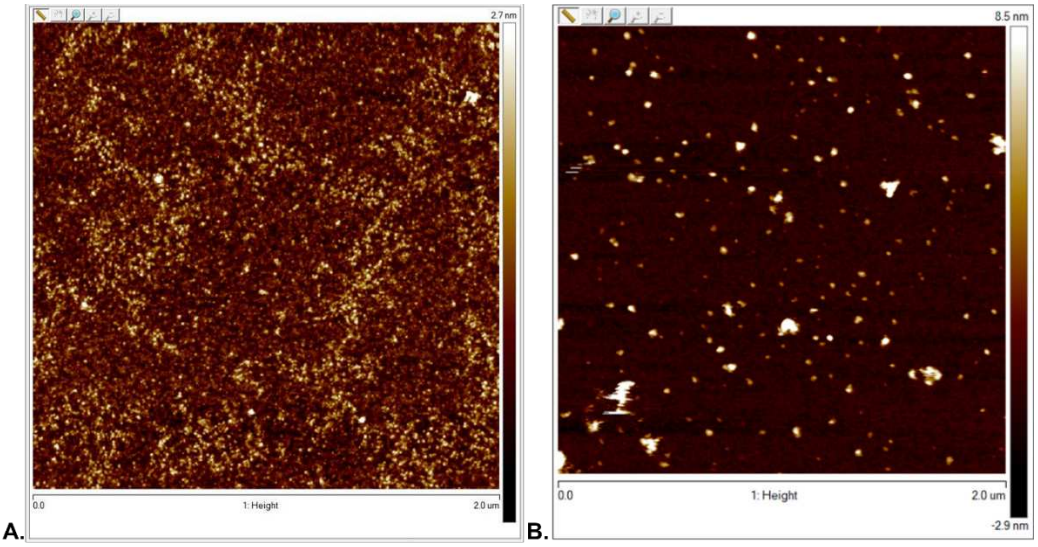

Figure 3. AFM image of the ColloidCuNPs (A) and CuNPs (B) layers. A gold mica substrate cover was applied for the deposition of coatings.

3.2.2. Surface morphology analysis

The layer coatings consisted of polyelectrolyte copper nanoparticles incorporating (PEI-CuNPs, PEI-ColloidCuNPs, PLL-CuNPs, and PLL-ColloidCuNPs) morphology was assessed (Figures 4, 5).

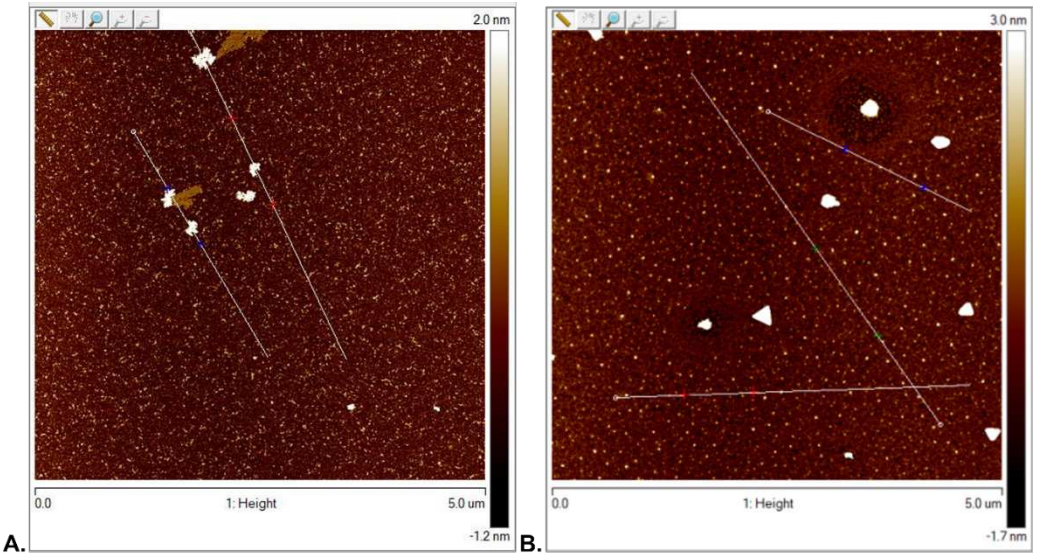

Figure 4. AFM image presenting designed layers placed on the gold mica substrate support. (A) The surface of the PLL-ColloidCuNPs coating; (B) the surface of PEI-ColloidCuNPs coating.

The layer PLL-ColloidCuNPs showed the structure with evenly marked tiny centers over the entire surface.

Polyethylenimine ColloidCuNPs incorporating showed an even structure with densely distributed centers. No branched structure was observed. The PLL-ColloidCuNPs and PEI-ColloidCuNPs layers' surface maximum roughness (R_{max}) [nm] value was 4.016 and 2.566, respectively (with profile height deviations from the mean line presented as root mean square (R_{ms}) [nm]: 0.376 and 0.39 respectively) (Figure 4).

 doi:10.20944/preprints202401.2054.v1

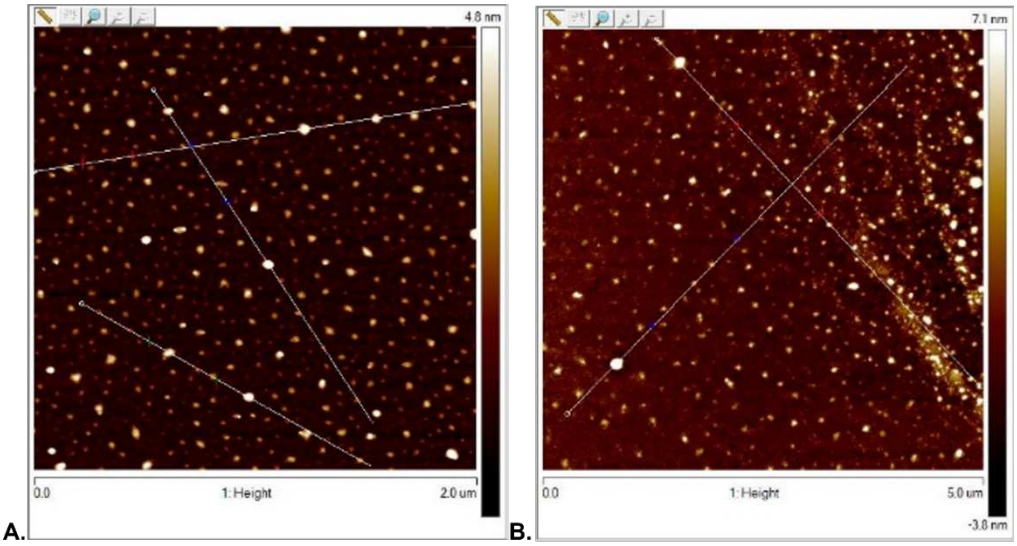

Figure 5. AFM image presents the layers deposited on the cover from the gold mica substrate. (A) The surface of the polylysine copper nanoparticles PLL-CuNPs incorporating coating; (B) the surface of the polyethylenimine copper nanoparticles PEI-CuNPs incorporating coating.

It was observed that the PLL-CuNPs layer exhibits the structure with evenly marked centers over the entire surface, analyzing the coatings incorporating CuNPs.

Polyethylenimine with CuNPs incorporated within showed an even structure with developed active centers presence due to the branched structure of PEI. The PLL-CuNPs and PEI-CuNPs layers R_{max} [nm]value was 2.123 and 9.426, respectively (with profile height deviations from the mean line presented as root mean square (R_{ms}) [nm]: 0.633 and 2.211 respectively) (Figure 5).

3.3. The Copper Nanoparticles Bacteriostatic Effect Evaluation

The bacteriostatic influence of CuNPs and ColloidCuNPs on the *E. coli* strain was assessed to examine their usability in supporting the biomaterials' bacteriostatic function (Figure 6). The results indicated the CuNPs bacteriostatic impact on the examined strain after 24-hour incubation. On the other hand, ColloidCuNPs did not exert bacteriostatic influence. Thus, CuNPs were selected for further evaluation due to their visible bacteriostatic functionality.

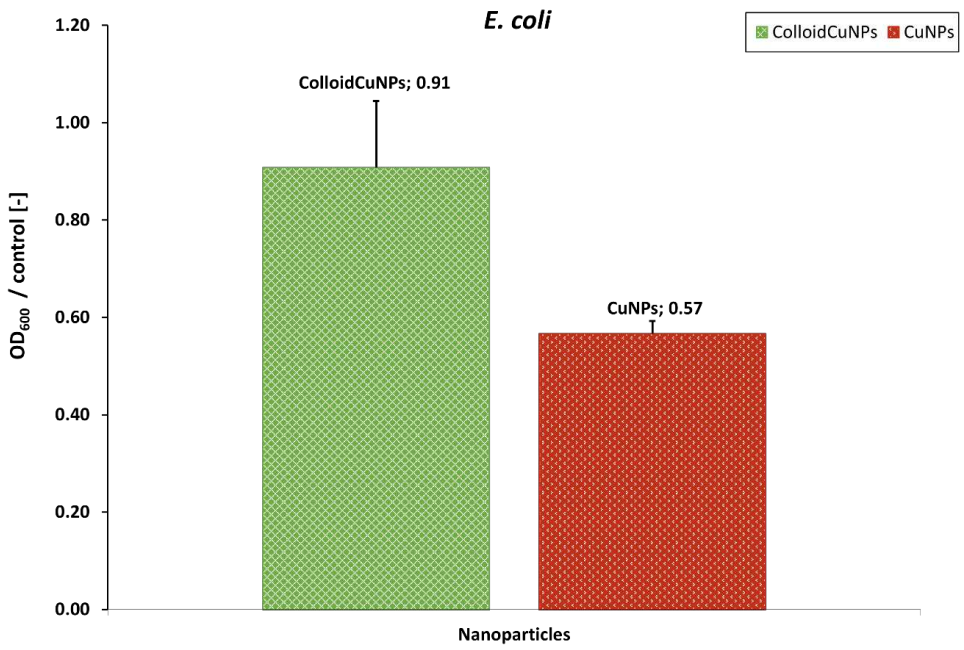

 doi:10.20944/preprints202401.2054.v1

Figure 6. The optical density (OD_{600}) rate (at λ= 600 nm) assessed for *Escherichia coli* bacterial strain maintained in the presence of the CuTONIK and CuNPs to the Control (*E. coli* maintained in lack of additions). The values are demonstrated as mean ± SD.

3.4. The Polyelectrolyte Layer Coatings CuNPs Incorporating Evaluation

3.4.1. SEM-EDX evaluation

Analyzing the nanocomposite material based on the PLL and PEI with CuNPs incorporated within, only the slight peak, which corresponds to Cu, was visible in EDX spectra of the PEI-CuNPs and PLL-CuNPs membrane, which might be caused by overlapping the signal with polyelectrolytes (Figure 7).

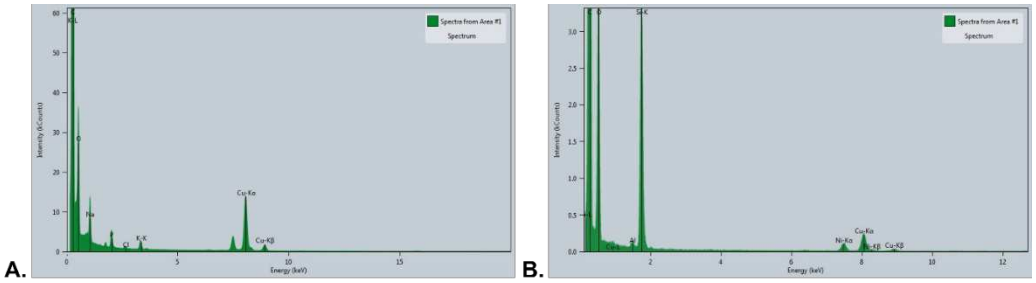

Figure 7. EDX spectra of PEI-CuNPs (A) and PLL-CuNPs (B) membrane with Cu peaks visible.

3.4.2. Water Contact Angle Studies

Characteristics of the material surface ensures the evaluation of its potential in biomedical applications. One key analyzed material properties is hydrophilic/hydrophobic interplay analysis [43]. The coating wettability was assessed by measuring the contact angle for water.

We tested coatings (1) based on poly-L-lysine, polylysine 10ppm incorporating CuNPs, polylysine 100ppm incorporating CuNPs, and (2) the coatings based on polyethylenimine; polyethylenimine 10ppm incorporating CuNPs; polyethylenimine 100ppm incorporating CuNPs.

The materials on the PLL basis alone and CuNPs incorporating showed hydrophilic properties with an average contact angle of 57.6 +/- 1.8. The materials on PEI basis alone and CuNPs incorporating show hydrophilic properties with an average contact angle of 63.2 +/- 4.42. There were no significant differences in the contact angle for the coatings of primary material and CuNPs at different share incorporating.

 doi:10.20944/preprints202401.2054.v1

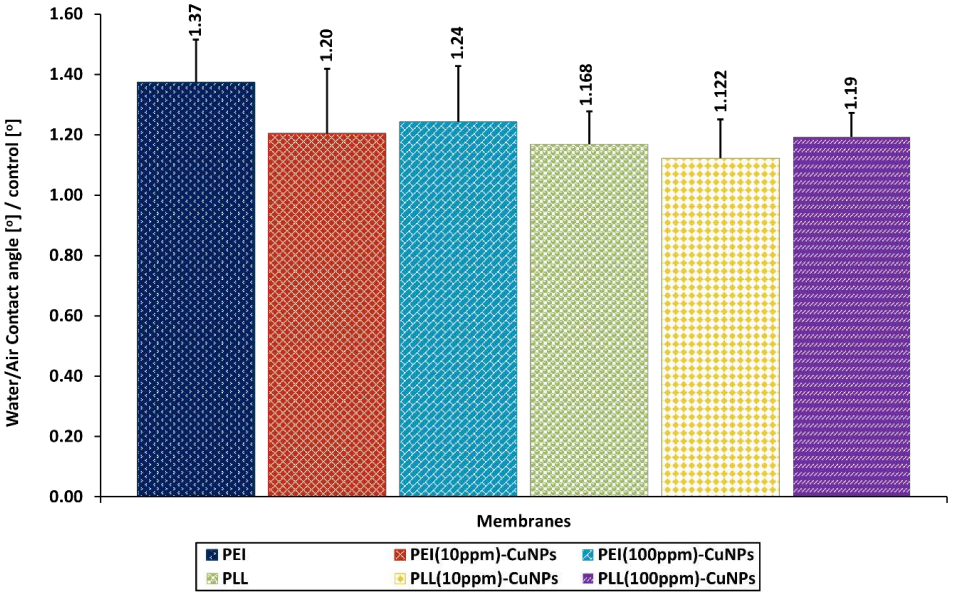

Figure 8. The rate of water contact angle of the layer coating surface to the Control (glass surface). Key to the symbols: PLL - polylysine; PLL_10ppm CuNPs -polylysine 10ppm CuNPs incorporating; PEI-polyethyleneimine; PEI_10ppm CuNPs – PEI 10ppm CuNPs incorporating. The presented values are mean± SD.

3.5. The functioning assessment of human lung cells in the presence of the layer coatings with CuNPs incorporated within.

3.5.1. MTT Evaluation

The developed layer coatings' cytotoxicity against human lung cell lines *in vitro* was assessed. Cells were maintained in the presence of the prepared coatings during a 10-day culture. The cells were maintained as a control without a coating layer presence in the culture for 10 days. MTT and fluorescence staining were applied to evaluate cell function and morphology.

The cells of human lung mitochondrial activity during culture with the addition of the examined coatings was assessed using an MTT assay.

After a 3-day culture on layer coating PLL, PLL+10ppm CuNPs, and PLL+100ppm CuNPs, the ratio relative to the control was comparable, and meanly 36% of the control value was observed. On the other hand, after 6 days of culture, the PLL, PLL+10ppm CuNPs layer coatings maintain A549 cells' function at a comparable level with the control. Moreover, on the 10th day of culture, the values obtained for layer coating PLL and PLL+10ppm CuNPs were comparable and exhibited comparable levels with the control. Nevertheless, the values obtained for the PLL+100ppm CuNPs layer coating were significantly lower compared to the control during the whole culture period (Figure 9).

 doi:10.20944/preprints202401.2054.v1

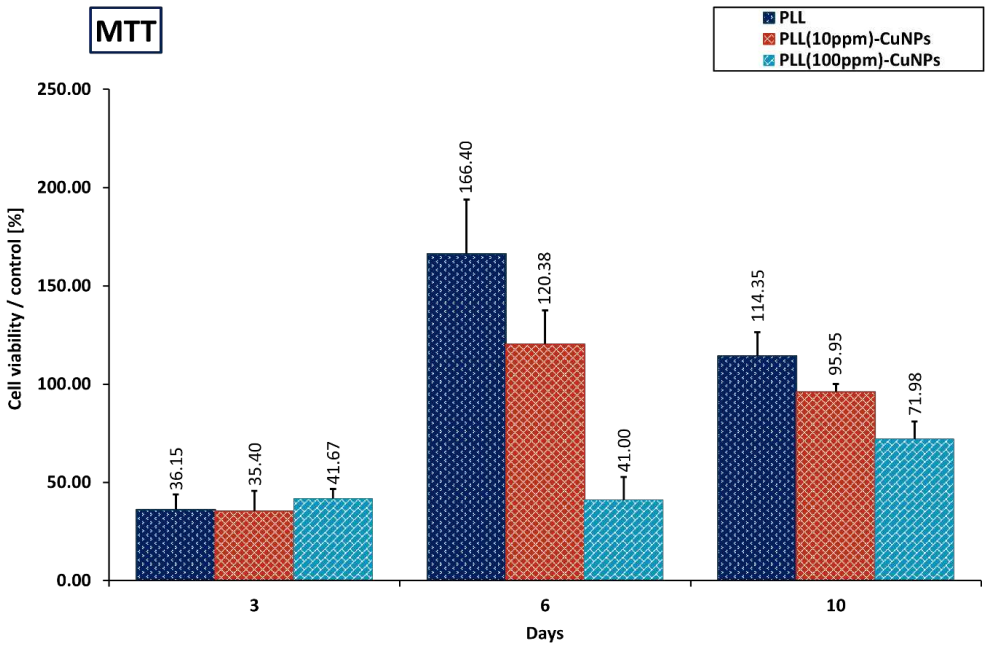

Figure 9. Evaluation of the mitochondrial activity of A549 cells immobilized on the PLL coating layer as a function of absorbance expressing the formazan production. The culture was maintained for 10 days. The values are in the form of the relative to the control ratio (mean ± SD). Key to the symbols: PLL-polylysine, PLL+10ppm CuNPs – polylysine 10ppm CuNPs incorporated, PLL+100ppm CuNPs – polylysine 100ppm CuNPs incorporated.

After a 3-day culture on layer coating PEI, PEI+10ppm CuNPs, and PEI+100ppm CuNPs, the ratio relative to the control was comparable, and meanly 45% of the control value was noted. On the contrary, after 6 days of culture, the PEI, PEI+10ppm CuNPs, and PEI+100ppm CuNPs layer coatings maintain A549 cells' function at a level that might become comparable to the control. On the 10th day of culture, the values obtained for layer coating PEI+10ppm CuNPs and PEI+100ppm CuNPs significantly declined compared to 6-day values (Figure 10).

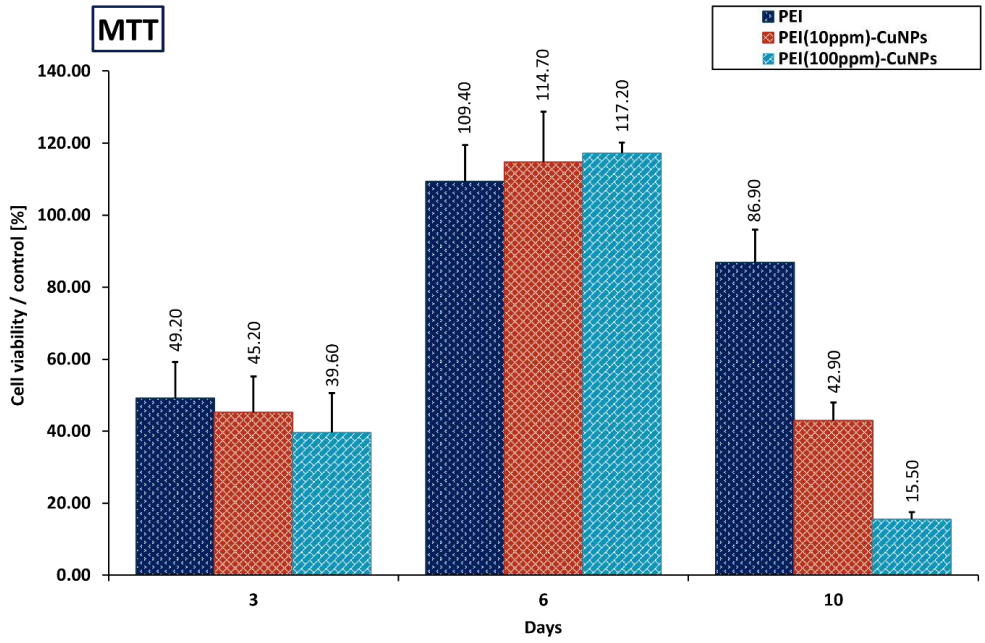

Figure 10. The A549 cells immobilized on the PEI coating layer mitochondrial activity expressed by absorbance representing formazan production. The culture was maintained for 10 days. The values

 doi:10.20944/preprints202401.2054.v1

are in the form of the relative to the control ratio (mean ± SD). Key to the symbols: PEI – polyethyleneimine, PEI+10ppm CuNPs – polyethylenimine 10ppm CuNPs incorporated, PEI+100ppm CuNPs – polyethyleneimine 100ppm CuNPs incorporated.

3.5.2. Fluorescence evaluation

The fluorescence microscopy evaluation performed during 1 week-culture showed that cells grown in the presence of PLL-CuNPs and PEI-CuNPs membranes exhibit the correct morphological structure (Figure 11). Based on the results, the analysis of the cells' morphology indicates spindle-shaped cells with fibroblastoid features. The numbers of cells observed on the surface of glass coverslips coated with PLL-CuNPs and PEI-CuNPs were comparable.

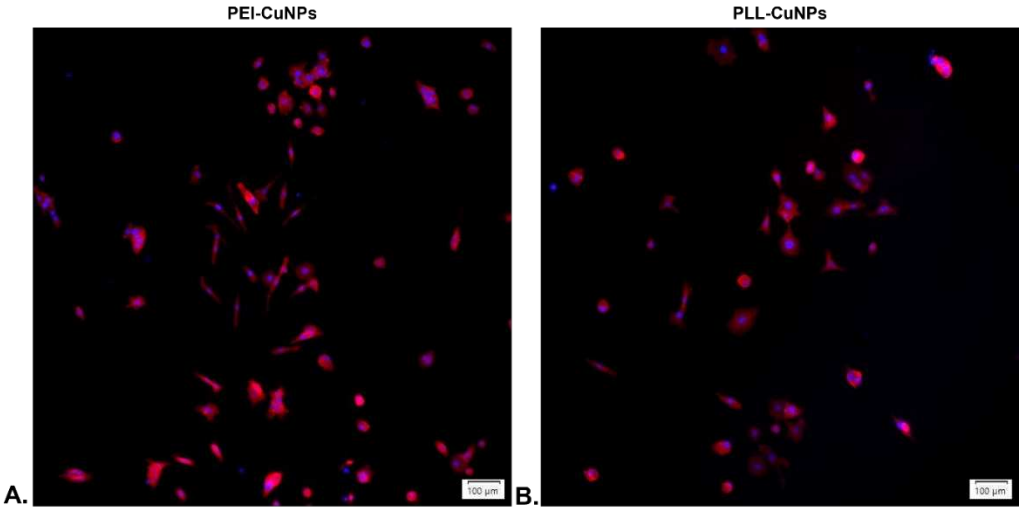

Figure 11. A549 cells maintained in the presence of PLL-10ppmCuNPs and PEI-10ppmCuNPs after a week of culture. Images were received using fluorescence microscopy.

3.6. Evaluation of the layer coatings CuNPs incorporating performance with E. coli

Examining the influence on the *E. coli* strain of the PEI-CuNPs incorporating CuNPs at share allowing A549 cells maintenance indicated that the presence of CuNPs in PEI-CuNPs deepens the bacteriostatic effect towards *E. coli* compared with PEI alone.

On the other hand, PLL-CuNPs did not exert bacteriostatic influence compared with control. (Figure 12.).

 doi:10.20944/preprints202401.2054.v1

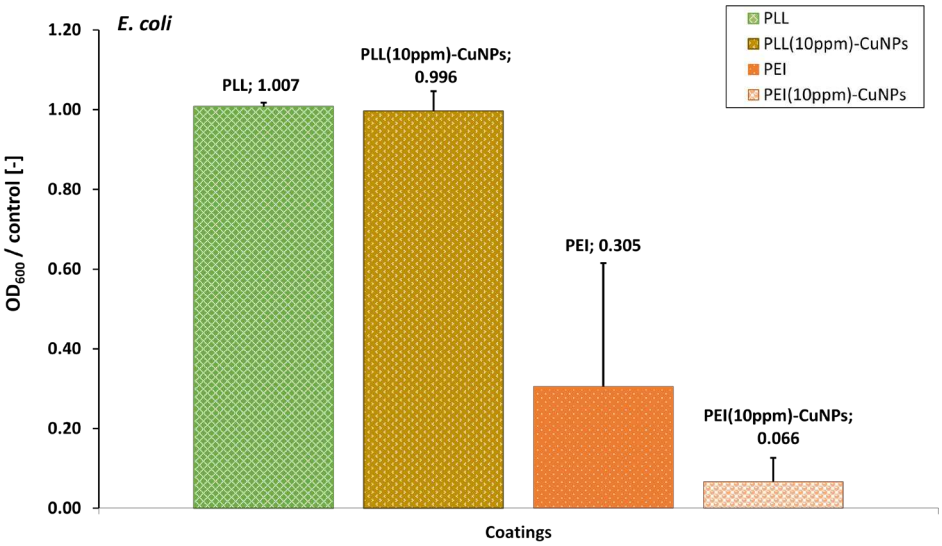

Figure 12. The optical density (OD_{600}) rate (at λ= 600 nm) for *Escherichia coli* bacterial strain after 24-hours incubation in the presence of the basis material PLL and PEI alone, as well as CuNPs incorporated layer coatings relative to the control (E. coli bacterial strain cultured alone). The values are the mean ± SD.

However, the overall charge of bacterial cells at physiological pH is negative due to the presence of the carboxylic groups in the lipoproteins within the bacterial membrane [44], and the electrostatic interaction with the opposite charge of copper ions released from nanoparticles is expected; it can be noted that CuNPs incorporation did not change the effect of PEI-CuNPs on *S. aureus* (Figure 13). The influence on *S. aureus* strains of PEI CuNPs incorporating indicated a similar effect as in the case of PE alone.

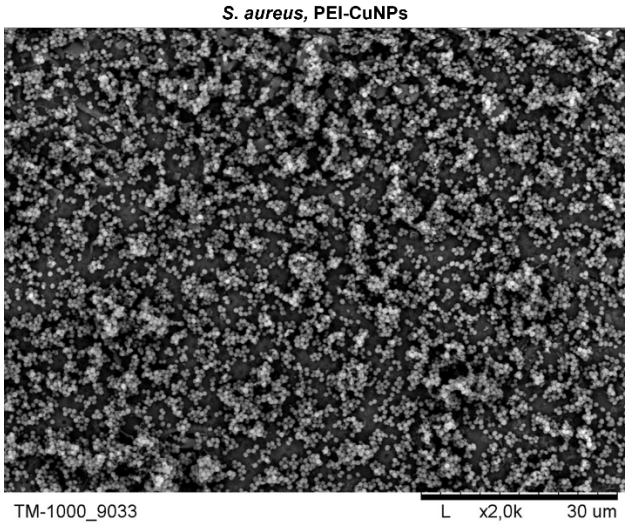

Figure 13. SEM picture of the *S. aureus* strains after 24h incubation in the presence of PEI-CuNPs layer coating.

4. Discussion

Biomaterials for supporting processes for biomedical purposes constitute an extensive area of research, including, e.g., facets of organ function preservation and tissue regeneration, antimicrobial

properties, and the possibilities of bridging the gap between basic research and commercial applications.

Virus-adsorbing polyelectrolyte base material was analyzed to determine whether it also has a bacteriostatic effect against Gram (+) and Gram (-) selected bacterial strains, and its function was verified in the configuration with incorporated copper nanoparticles.

Assuming that the isoelectric point (pI) of the spike glycoprotein for SARS-CoV-2 is equal to 6.24 [45], in the physiological environment (pH = 7.2), the stalk part is negatively charged. Consequently, positively charged groups of antiviral material could interact electrostaticly with it.

Moreover, reports for Gram (-) *Escherichia coli* show that the negative charge density of the lipopolysaccharide-coated outer surface is higher than the protein surface layer of Gram (+) bacterial cells [46], which should make it much easier for such a material to adsorb Gram (-) bacterial cells.

Nevertheless, PLL did not exert the bacteriostatic effect on both Gram (+) and Gram (-) strains, which may result from the interaction of polylysine residues with the bacterial membrane being too weak. On the other hand, the 25nm CuNPs involving PEI-based nanocomposite layer coating exerted a bacteriostatic effect against *E. coli* without delimiting the A549 cells' function in the aspect of mitochondrial activity up to a week of culture. The changes in the mitochondrial activity of cells during the 10 days of culture on produced layer coatings may reflect the stress response induced by the involvement of the CuNPs, resulting in changes in intra- and inter-mitochondrial redox-environment; as a consequence, ROS is released. Intracellular dissolution of Cu^{2+} might enhance this effect.

Although the proposed layer coating fits into the field of biomaterials and meets specific criteria, it should be noted that an ideal biomaterial does not exist, and it is necessary to consider what biological material it should cooperate with/is expected to cooperate with and whether there are certain specific bacterial strains against which it should have a bactericidal effect. Moreover, finding a balance between the cytotoxic and bacteriostatic effects is necessary. Furthermore, it is necessary to determine the expected surface properties for individual cooperation with the intended recipient.

The size of the nanoparticles the biological material comes into contact with also plays a role. For example, Jing et al. have analyzed the toxicity of 9.2nm copper oxide nanoparticles (CuONPs) on human bronchial epithelial cells (HBEC) as well as lung adenocarcinoma cells (A549 cells) by applying an exposure system based on *in vitro* air-liquid interface (ALI), observed their cytotoxic effect on cells [47].

Some other authors reported that Cu/CuO NPs of size smaller than 20 nm suppressed the proliferation and viability of regular (WI-38) and carcinoma (A549) human lung cell lines [48].

Additionally, reports submitted for the A549 human lung cell line compare the *in vitro* cytotoxicity of 4 and 24nm CuONPs [49]. The authors observed significantly higher cytotoxicity for 24nm CuONPs than 4 nm ones, which leads us to consider the balance between nanoparticle size and the NPs cell-entry rate.

The result suggests that the 100ppm share of CuNPs in produced layer coatings excludes their use to maintain the A549 cell functions. The 10ppm share of CuNPs in nanocomposite coating allows for obtaining the balance between the cytotoxicity and bacteriostatic effect. To sum up, it is crucial to understand the antimicrobial mechanisms as separate antiviral and antibacterial functions of individual copper nanoparticles, considering their size and phase composition. This function determines the potential of copper nanoparticles for biomedical purposes and may constitute a starting point for ongoing research on their use for therapeutic purposes.

5. Conclusions

In summary, CuNPs involving PEI-based layer coating involving 25nm CuNPs at 10ppm share with topography, ensuring an even contact surface for epithelial tissue cells interface and exerting bacteriostatic effect against *E. coli* without delimiting the A549 cells function can be considered as an element of the system components for medical devices for maintaining the human lung cells' function.

Author Contributions: Conceptualization, A.L., A.G. and L.G.; methodology, A.L., A.G. and L.G.; validation, L.G.; formal analysis, L.G., A.K.; investigation, A.L., A.G., M.A, M.S., M.D., E.G.; writing—original draft preparation, A.K. and L.G.; writing—review and editing, A.K. and L.G.; visualization, A.K.; supervision, L.G.

All authors have read and agreed to the published version of the manuscript.

Funding: This research received no external funding

Data Availability Statement: Data is unavailable.

Conflicts of Interest: The authors declare no conflicts of interest.

References

1. Costa, N.N.; de Faria Lopes, L.; Ferreira, D.F.; de Prado, E.M.L.; Severi, J.A.; Resende, J.A.; de Paula Careta, F.; Ferreira, M.C.P.; Carreira, L.G.; de Souza, S.O.L.; et al. Polymeric films containing pomegranate peel extract based on PVA/starch/PAA blends for use as wound dressing: In vitro analysis and physicochemical evaluation. *Mater. Sci. Eng. C* **2020**, *109*, 110643, doi:10.1016/J.MSEC.2020.110643.
2. Stricker, P.E.F.; de Souza Dobuchak, D.; Irioda, A.C.; Mogharbel, B.F.; Franco, C.R.C.; de Souza Almeida Leite, J.R.; de Araújo, A.R.; Borges, F.A.; Herculano, R.D.; de Oliveira Graeff, C.F.; et al. Human mesenchymal stem cells seeded on the natural membrane to neurospheres for cholinergic-like neurons. *Membranes (Basel).* **2021**, *11*, 598, doi:10.3390/MEMBRANES11080598/S1.
3. Dziedzic, D.S.M.; Mogharbel, B.F.; Irioda, A.C.; Stricker, P.E.F.; Perussolo, M.C.; Franco, C.R.C.; Chang, H.W.; Abdelwahid, E.; de Carvalho, K.A.T. Adipose-Derived Stromal Cells and Mineralized Extracellular Matrix Delivery by a Human Decellularized Amniotic Membrane in Periodontal Tissue Engineering. *Membranes (Basel).* **2021**, *11*, doi:10.3390/MEMBRANES11080606.
4. Yang, C.; Yang, C.; Chen, Y.; Liu, J.; Liu, Z.; Chen, H.J. The trends in wound management: Sensing, therapeutic treatment, and "theranostics." *J. Sci. Adv. Mater. Devices* 2023, *8*.
5. Veiga, A.S.; Schneider, J.P. Antimicrobial hydrogels for the treatment of infection. *Pept. Sci.* **2013**, *100*, 637–644, doi:10.1002/BIP.22412.
6. Ponco, A.; Helmiyati, H. Hydrogel of carboxymethyl cellulose and polyvinyl alcohol modified by CuNPs as antibacterial in wound dressing. *AIP Conf. Proc.* **2020**, *2242*, 040009, doi:10.1063/5.0008096.
7. Wang, F.; Zhang, W.; Li, H.; Chen, X.; Feng, S.; Mei, Z. How Effective are Nano-Based Dressings in Diabetic Wound Healing? A Comprehensive Review of Literature. *Int. J. Nanomedicine* **2022**, *17*, 2097–2119, doi:10.2147/IJN.S361282.
8. Annabi, N.; Rana, D.; Shirzaei Sani, E.; Portillo-Lara, R.; Gifford, J.L.; Fares, M.M.; Mithieux, S.M.; Weiss, A.S. Engineering a sprayable and elastic hydrogel adhesive with antimicrobial properties for wound healing. *Biomaterials* **2017**, *139*, doi:10.1016/j.biomaterials.2017.05.011.
9. Tashkandi, H. Honey in wound healing: An updated review. *Open Life Sci.* **2021**, *16*, 1091, doi:10.1515/BIOL-2021-0084.
10. Crisan, M.C.; Teodora, M.; Lucian, M. Copper Nanoparticles: Synthesis and Characterization, Physiology, Toxicity and Antimicrobial Applications. *Appl. Sci. 2022, Vol. 12, Page 141* **2021**, *12*, 141, doi:10.3390/APP12010141.
11. Bruna, T.; Maldonado-Bravo, F.; Jara, P.; Caro, N. Silver Nanoparticles and Their Antibacterial Applications. *Int. J. Mol. Sci. 2021, Vol. 22, Page 7202* **2021**, *22*, 7202, doi:10.3390/IJMS22137202.
12. Das, A.; Ash, D.; Fouda, A.Y.; Sudhahar, V.; Kim, Y.M.; Hou, Y.; Hudson, F.Z.; Stansfield, B.K.; Caldwell, R.B.; McMenamin, M.; et al. Cysteine oxidation of copper transporter CTR1 drives VEGFR2 signalling and angiogenesis. *Nat. Cell Biol.* **2022**, *24*, 35–50, doi:10.1038/S41556-021-00822-7.
13. Sudheesh Kumar, P.T.; Lakshmanan, V.K.; Anilkumar, T. V.; Ramya, C.; Reshmi, P.; Unnikrishnan, A.G.; Nair, S. V.; Jayakumar, R. Flexible and microporous chitosan hydrogel/nano ZnO composite bandages for wound dressing: In vitro and in vivo evaluation. *ACS Appl. Mater. Interfaces* **2012**, *4*, 2618–2629, doi:10.1021/AM300292V/ASSET/IMAGES/MEDIUM/AM-2012-00292V_0007.GIF.
14. Khashan, K.S.; Sulaiman, G.M.; Mahdi, R. Preparation of iron oxide nanoparticles-decorated carbon nanotube using laser ablation in liquid and their antimicrobial activity. *Artif. cells, nanomedicine, Biotechnol.* **2017**, *45*, 1699–1709, doi:10.1080/21691401.2017.1282498.
15. Nosrati, H.; Heydari, M.; Khodaei, M. Cerium oxide nanoparticles: Synthesis methods and applications in wound healing. *Mater. Today Bio* **2023**, *23*, 2590–0064, doi:10.1016/J.MTBIO.2023.100823.
16. Kamoun, E.A.; Kenawy, E.R.S.; Chen, X. A review on polymeric hydrogel membranes for wound dressing applications: PVA-based hydrogel dressings. *J. Adv. Res.* **2017**, *8*, 217–233, doi:10.1016/J.JARE.2017.01.005.
17. Vijayakumar, G.; Kim, H.J.; Rangarajulu, S.K. In Vitro Antibacterial and Wound Healing Activities Evoked by Silver Nanoparticles Synthesized through Probiotic Bacteria. *Antibiotics* **2023**, *12*, doi:10.3390/ANTIBIOTICS12010141/S1.

18. Soliman, W.E.; Elsewedy, H.S.; Younis, N.S.; Shinu, P.; Elsawy, L.E.; Ramadan, H.A. Evaluating Antimicrobial Activity and Wound Healing Effect of Rod-Shaped Nanoparticles. *Polymers (Basel).* **2022**, *14*, doi:10.3390/POLYM14132637.
19. Chandrakala, V.; Aruna, V.; Angajala, G. Review on metal nanoparticles as nanocarriers: current challenges and perspectives in drug delivery systems. *Emergent Mater. 2021 56* **2022**, *5*, 1593–1615, doi:10.1007/S42247-021-00335-X.
20. Ostaszewska, T.; Śliwiński, J.; Kamaszewski, M.; Sysa, P.; Chojnacki, M. Cytotoxicity of silver and copper nanoparticles on rainbow trout (Oncorhynchus mykiss) hepatocytes. *Environ. Sci. Pollut. Res.* **2018**, *25*, 908–915, doi:10.1007/S11356-017-0494-0/FIGURES/9.
21. Salvo, J.; Sandoval, C.; Schencke, C.; Acevedo, F.; del Sol, M. Healing Effect of a Nano-Functionalized Medical-Grade Honey for the Treatment of Infected Wounds. *Pharm. 2023, Vol. 15, Page 2187* **2023**, *15*, 2187, doi:10.3390/PHARMACEUTICS15092187.
22. Deokar, A.R.; Perelshtein, I.; Saibene, M.; Perkas, N.; Mantecca, P.; Nitzan, Y.; Gedanken, A. Antibacterial and In Vivo Studies of a Green, One-Pot Preparation of Copper/Zinc Oxide Nanoparticle-Coated Bandages. *Membranes (Basel).* **2021**, *11*, doi:10.3390/MEMBRANES11070462.
23. Kruk, T.; Gołda-Cępa, M.; Szczepanowicz, K.; Szyk-Warszyńska, L.; Brzychczy-Włoch, M.; Kotarba, A.; Warszyński, P. Nanocomposite multifunctional polyelectrolyte thin films with copper nanoparticles as the antimicrobial coatings. *Colloids Surf. B. Biointerfaces* **2019**, *181*, 112–118, doi:10.1016/J.COLSURFB.2019.05.014.
24. Wang, Y.; Zhang, W.; Yao, Q. Copper-based biomaterials for bone and cartilage tissue engineering. *J. Orthop. Transl.* **2021**, *29*, 60–71, doi:10.1016/J.JOT.2021.03.003.
25. Xie, H.; Kang, Y. Role of copper in angiogenesis and its medicinal implications. *Curr. Med. Chem.* **2009**, *16*, 1304–1314, doi:10.2174/092986709787846622.
26. Zhou, W.; Zi, L.; Cen, Y.; You, C.; Tian, M. Copper Sulfide Nanoparticles-Incorporated Hyaluronic Acid Injectable Hydrogel With Enhanced Angiogenesis to Promote Wound Healing. *Front. Bioeng. Biotechnol.* **2020**, *8*, 543970, doi:10.3389/FBIOE.2020.00417/BIBTEX.
27. Tripathi, A.; Saravanan, S.; Pattnaik, S.; Moorthi, A.; Partridge, N.C.; Selvamurugan, N. Bio-composite scaffolds containing chitosan/nano-hydroxyapatite/nano-copper-zinc for bone tissue engineering. *Int. J. Biol. Macromol.* **2012**, *50*, 294–299, doi:10.1016/J.IJBIOMAC.2011.11.013.
28. Liu, C.; Fu, X.; Pan, H.; Wan, P.; Wang, L.; Tan, L.; Wang, K.; Zhao, Y.; Yang, K.; Chu, P.K. Biodegradable Mg-Cu alloys with enhanced osteogenesis, angiogenesis, and long-lasting antibacterial effects. *Sci. Reports 2016 61* **2016**, *6*, 1–17, doi:10.1038/srep27374.
29. Alizadeh, S.; Seyedalipour, B.; Shafieyan, S.; Kheime, A.; Mohammadi, P.; Aghdami, N. Copper nanoparticles promote rapid wound healing in acute full thickness defect via acceleration of skin cell migration, proliferation, and neovascularization. *Biochem. Biophys. Res. Commun.* **2019**, *517*, 684–690, doi:10.1016/J.BBRC.2019.07.110.
30. Wu, C.; Zhou, Y.; Xu, M.; Han, P.; Chen, L.; Chang, J.; Xiao, Y. Copper-containing mesoporous bioactive glass scaffolds with multifunctional properties of angiogenesis capacity, osteostimulation and antibacterial activity. *Biomaterials* **2013**, *34*, 422–433, doi:10.1016/J.BIOMATERIALS.2012.09.066.
31. Rath, S.N.; Brandl, A.; Hiller, D.; Hoppe, A.; Gbureck, U.; Horch, R.E.; Boccaccini, A.R.; Kneser, U. Bioactive Copper-Doped Glass Scaffolds Can Stimulate Endothelial Cells in Co-Culture in Combination with Mesenchymal Stem Cells. *PLoS One* **2014**, *9*, e113319, doi:10.1371/JOURNAL.PONE.0113319.
32. Ryan, E.J.; Ryan, A.J.; González-Vázquez, A.; Philippart, A.; Ciraldo, F.E.; Hobbs, C.; Nicolosi, V.; Boccaccini, A.R.; Kearney, C.J.; O'Brien, F.J. Collagen scaffolds functionalised with copper-eluting bioactive glass reduce infection and enhance osteogenesis and angiogenesis both in vitro and in vivo. *Biomaterials* **2019**, *197*, 405–416, doi:10.1016/J.BIOMATERIALS.2019.01.031.
33. Miola, M.; Cochis, A.; Kumar, A.; Arciola, C.R.; Rimondini, L.; Verné, E. Copper-Doped Bioactive Glass as Filler for PMMA-Based Bone Cements: Morphological, Mechanical, Reactivity, and Preliminary Antibacterial Characterization. *Mater. 2018, Vol. 11, Page 961* **2018**, *11*, 961, doi:10.3390/MA11060961.
34. Grass, G.; Rensing, C.; Solioz, M. Metallic copper as an antimicrobial surface. *Appl. Environ. Microbiol.* **2011**, *77*, 1541–1547, doi:10.1128/AEM.02766-10.
35. Ameh, T.; Sayes, C.M. The potential exposure and hazards of copper nanoparticles: A review. *Environ. Toxicol. Pharmacol.* **2019**, *71*, doi:10.1016/J.ETAP.2019.103220.
36. Lin, R.; Deng, C.; Li, X.; Liu, Y.; Zhang, M.; Qin, C.; Yao, Q.; Wang, L.; Wu, C. Copper-incorporated bioactive glass-ceramics inducing anti-inflammatory phenotype and regeneration of cartilage/bone interface. *Theranostics* **2019**, *9*, 6300–6313, doi:10.7150/THNO.36120.
37. Kumari, S.; Mishra, A.; Singh, D.; Li, C.; Srivastava, P. In-vitro Studies on Copper Nanoparticles and Nano-hydroxyapatite Infused Biopolymeric Composite Scaffolds for Bone Bioengineering Applications. *Biotechnol. Bioprocess Eng.* **2023**, *28*, 162–180, doi:10.1007/S12257-022-0236-0/METRICS.
38. Kornblatt, A.P.; Nicoletti, V.G.; Travaglia, A. The neglected role of copper ions in wound healing. *J. Inorg. Biochem.* **2016**, *161*, 1–8, doi:10.1016/J.JINORGBIO.2016.02.012.

39. Gorel, O.; Hamuda, M.; Feldman, I.; Kucyn-Gabovich, I. Enhanced healing of wounds that responded poorly to silver dressing by copper wound dressings: Prospective single arm treatment study. *Heal. Sci. Reports* **2024**, *7*, e1816, doi:10.1002/HSR2.1816.
40. Kotton, D.N.; Morrisey, E.E. Lung regeneration: mechanisms, applications and emerging stem cell populations. *Nat. Med.* **2014**, *20*, 822–832, doi:10.1038/NM.3642.
41. Lucchini, A.C.; Gachanja, N.N.; Rossi, A.G.; Dorward, D.A.; Lucas, C.D. Epithelial Cells and Inflammation in Pulmonary Wound Repair. *Cells 2021, Vol. 10, Page 339* **2021**, *10*, 339, doi:10.3390/CELLS10020339.
42. Grzeczkowicz, A.; Lipko, A.; Kwiatkowska, A.; Strawski, M.; Bącal, P.; Więckowska, A.; Granicka, L.H. Polyelectrolyte Membrane Nanocoatings Aimed at Personal Protective and Medical Equipment Surfaces to Reduce Coronavirus Spreading. *Membr. 2022, Vol. 12, Page 946* **2022**, *12*, 946, doi:10.3390/MEMBRANES12100946.
43. Corsaro, C.; Mallamace, D.; Neri, G.; Fazio, E. Hydrophilicity and hydrophobicity: Key aspects for biomedical and technological purposes. *Phys. A Stat. Mech. its Appl.* **2021**, *580*, 126189, doi:10.1016/J.PHYSA.2021.126189.
44. Stoimenov, P.K.; Klinger, R.L.; Marchin, G.L.; Klabunde, K.J. Metal Oxide Nanoparticles as Bactericidal Agents. *Langmuir* **2002**, *18*, 6679–6686, doi:10.1021/LA0202374.
45. Scheller, C.; Krebs, F.; Minkner, R.; Astner, I.; Gil-Moles, M.; Wätzig, H. Physicochemical properties of SARS-CoV-2 for drug targeting, virus inactivation and attenuation, vaccine formulation and quality control. *Electrophoresis* 2020, *41*.
46. Wilhelm, M.J.; Sharifian Gh., M.; Wu, T.; Li, Y.; Chang, C.M.; Ma, J.; Dai, H.L. Determination of bacterial surface charge density via saturation of adsorbed ions. *Biophys. J.* **2021**, *120*, 2461–2470, doi:10.1016/J.BPJ.2021.04.018.
47. Jing, X.; Park, J.H.; Peters, T.M.; Thorne, P.S. Toxicity of copper oxide nanoparticles in lung epithelial cells exposed at the air-liquid interface compared with in vivo assessment. *Toxicol. In Vitro* **2015**, *29*, 502–511, doi:10.1016/J.TIV.2014.12.023.
48. Fahmy, H.M.; Ebrahim, N.M.; Gaber, M.H. In-vitro evaluation of copper/copper oxide nanoparticles cytotoxicity and genotoxicity in normal and cancer lung cell lines. *J. Trace Elem. Med. Biol.* **2020**, *60*, doi:10.1016/J.JTEMB.2020.126481.
49. Wongrakpanich, A.; Mudunkotuwa, I.A.; Geary, S.M.; Morris, A.S.; Mapuskar, K.A.; Spitz, D.R.; Grassian, V.H.; Salem, A.K. Size-dependent cytotoxicity of copper oxide nanoparticles in lung epithelial cells. *Environ. Sci. Nano* **2016**, *3*, 365–374, doi:10.1039/C5EN00271K.